Applied Radiation and Isotopes 69 (2011) 1732–1736

Contents lists available at ScienceDirect

Applied Radiation and Isotopes

journal homepage: www.elsevier.com/locate/apradiso

In vitro studies of cellular response to DNA damage induced by boron neutron capture therapy

M. Perona [a,e], O. Pontiggia [d,e], M. Carpano [a], L. Thomasz [a], S. Thorp [b], E. Pozzi [c], M. Simian [d,e], S. Kahl [g], G. Juvenal [a,e], M. Pisarev [a,e,f], A. Dagrosa [a,e,*]

[a] Department of Radiobiology, Av. General Paz 1499, San Martin (1560), Argentina
[b] Department of Instrumentation and Control, Av. General Paz 1499, San Martin (1560), Argentina
[c] RA-3 Reactor, National Atomic Energy Commission (CNEA), Av. General Paz 1499, San Martin (1560), Argentina
[d] Institute of Oncology "Angel H. Roffo", Av. San Martín 5481, (1417) Cdad. de Buenos Aires, Argentina
[e] National Research Council of Argentina (CONICET), Rivadavia 1917, (1033) Buenos Aires, Argentina
[f] Department of Biochemistry, UBA, School of Medicine, Argentina
[g] Department of Pharmaceutical Chemistry, University of California, San Francisco, USA

ARTICLE INFO

Available online 8 April 2011

Keywords:
Damage
DNA
Cell cycle
NHEJ

ABSTRACT

The aim of these studies was to evaluate the mechanisms of cellular response to DNA damage induced by BNCT. Thyroid carcinoma cells were incubated with ^{10}BPA or ^{10}BOPP and irradiated with thermal neutrons. The surviving fraction, the cell cycle distribution and the expression of p53 and Ku70 were analyzed. Different cellular responses were observed for each irradiated group. The decrease of Ku70 in the neutrons +BOPP group could play a role in the increase of sensitization to radiation.

1. Introduction

Boron neutron capture therapy (BNCT) is a high linear energy transfer (LET) radiotherapy for cancer, based on the nuclear reaction that occurs when ^{10}B, a nonradioactive isotope of natural elemental boron, reacts with low energy thermal neutrons to produce an alpha particle (^{4}He) and a ^{7}Li nucleus. Both particles have a range comparable to the diameter of a cell causing tumor cell death without significant damage to the surrounding normal tissues, provided that the boron-carrier compound accumulates preferentially in tumor cells (Coderre and Morris, 1999). BNCT has been then used in clinical trials for the treatment of high grade gliomas, cutaneous melanomas and its brain metastases using as boron carriers, p-boronophenylalanine (^{10}BPA) and sodium borocaptate (^{10}BSH) (Altieri et al., 2009). Also, in the last years, this therapeutic modality has been applied in the treatment of head and neck tumors (Wittig et al., 2009; Kato et al., 2009).

We have performed studies on a human anaplastic thyroid carcinoma cell line using as a carrier of boron, ^{10}BPA and also tetrakis-carborane carboxylate ester of 2,4-bis (α,β-dihydroxyethyl)-deutero-porphyrin IX (BOPP), both *in vitro* and after being transplanted to nude mice (Dagrosa et al., 2003, 2007). These studies were very encouraging; however little is known about the mechanisms that play a role in the tumor damage produced by BNCT. The DNA molecule is the principal biological target that conduces to cell death. The high LET radiation produces mostly DNA double strand breaks (DSBs) and it is normal to observe chromosomal aberrations and its cytoplasmic derivates, the micronuclei (MN) (Norppa and Falck, 2003). Cell cycle regulation and repair mechanisms such as homologous recombination (HR) and nonhomologous end-joining (NHEJ) are important determinants of ionizing radiation sensitivity. A common cellular response to DNA-damaging agents is the activation of cell cycle checkpoints. One of the key proteins in the checkpoint pathway is the tumor suppressor gene p53, which coordinates DNA repair with cell cycle progression and apoptosis (Pawlik and Keyomarsi, 2004). Normally, DNA double strand breaks activate Ku proteins, which bind to the area of DNA breakage. Ku70 protein is involved in the repair of DNA double strand breaks via NHEJ pathway and can also play an important role in the apoptosis (Ochi et al., 2010).

Previously we have shown that both cytotoxic and genotoxic effects produced in the cells treated by BNCT are different and higher than those produced in cells irradiated with the gamma irradiation. The number of micronuclei per cell increases as a function of the total physical dose following a sigmoidal model (Dagrosa et al., 2011). In the present work we evaluated in thyroid carcinoma cells the mechanisms of cellular response to DNA damage induced by BNCT and compared them with the conventional gamma radiation.

* Corresponding author at: Department of Radiobiology, National Atomic Energy Commission (CNEA), Av. General Paz 1499, San Martin (1560), Argentina.
Tel.: +54 11 6772 7966; fax: +54 11 6772 7121.
E-mail address: dagrosa@cnea.gov.ar (A. Dagrosa).

0969-8043/$ - see front matter © 2011 Published by Elsevier Ltd.
doi:10.1016/j.apradiso.2011.03.044

2. Material and method

2.1. Cell line

Human cell line of follicular thyroid carcinoma (WRO) was grown and maintained in RPMI 1640 medium supplemented with 10% de FBS, under 5% CO_2 atmosphere at 37 °C.

2.2. Experimental design

Exponentially growing cells were distributed in the following groups: (1) ^{10}BPA+neutrons: cells were incubated with ^{10}BPA at a dose of 10 μg ^{10}B/mL (0.925 M) during 16 h before irradiation; (2) ^{10}BOPP (2,4-bis (α,β-dihydroxyethyl)-deutero-porphyrin IX)+ neutrons: cells were incubated with ^{10}BOPP at a dose of 10 μg ^{10}B/mL (33 μg/mL) during 16 h before irradiation; (3) Neutrons (N) and (4) Gamma. A control group without irradiation for each treatment was added: Control (C), C BPA and C BOPP.

2.3. Dosimetry

Cells were gamma irradiated using a ^{60}Co source (1 Gy/min) and neutron irradiated at the thermal column of the RA-3 reactor (Miller et al., 2009). This is an 8 MW reactor, located in Ezeiza, Argentina where a highly thermalized and homogenous irradiation field is available. Thermal flux is near $(8.5 \pm 0.7) \times 10^9$ n/(cm^2 s), the cadmium ratio is 4100 for gold foils, which allows neglecting fast neutron dose, and the gamma dose rate is approximately 6.0 ± 0.2 Gy/h. In both cases, different time lapses were selected in order to achieve total physical doses ranging between 0.3 and 5 Gy ($\pm$10%).

2.4. Cell surviving assay

For cell viability evaluation, 2000 cells were seeded with 200 μL of RPMI medium and 10% FBS in 96-wells plates. Four different wells were seeded per treatment. After irradiation, the medium was changed and the cells were cultured at 37 °C. The medium was changed again at day 4 after irradiation and 20 μL of vital dye 3-(4,5-dimethylthiazol-2-yl)-2,5 diphenyltetrazolium-bromide (MTT) [Sigma 128] 0.5% w/v in PBS was added. Absorbance was measured at 540 nm.

2.5. Protein expression assay

For *Western blot* analysis, the cells were incubated at 37 °C for 24 and 48 h after irradiation. Cells were washed twice in cold PBS, scrapped and centrifuged. The PBS was removed and the pellet was lysed in 100 μL of RIPA buffer (50 mM Tris–HCl, pH 7.2, 150 mM NaCl, 1% Nonidet P-40, 1% sodium deoxycholate and 0.1% SDS) containing protease inhibitors. The cell lysate was cleared by centrifugation and the supernatant was used as a total cellular protein extract. Protein concentration was determined by Bradford protein assay (BioRad).

From each sample 60 μg of total protein was loaded into a 12% SDS-polyacrylamide gel and electrophoresed at 90 V for 2 h. The separated proteins were transferred to a *Hybond-P* membrane (Amersham) in transfer buffer (25 mM Tris-base, 192 mM glycine, 20% methanol and 0.05% SDS) at 100 V for 1 h at 4 °C. The membrane was incubated in blocking solution (5% nonfat milk in TBST: 30 mM Tris–HCl, pH 7.4; 150 mM NaCl; and 0.05% Tween-20) and probed with mouse antibodies raised against p53 (Clone DO-7, Pharmingen) and Ku70 (Calbiochem). Beta-Actin monoclonal antibody (Clone AC-15, Sigma) was used as a loading control. The membrane was washed and incubated with the secondary antibody (anti-mouse antibody conjugated to horseradish peroxidase, Promega). The bands were visualized by chemiluminescence after addition of substrate (ECL detection kit, Amersham) and exposed to autoradiograph films. Semi-quantitative analysis was obtained after the films were scanned with a densitometer to determine the density of each band. The relative optical density (OD) was obtained by dividing the density of each band by the Beta-Actin density.

2.6. Cell cycle analysis

For cell cycle, 10^6 cells were washed three times with ice-cold PBS and fixed in absolute ethanol at −20 °C, O/N. Cell pellets were resuspended in a staining solution of PBS containing 60 μg/mL propidium iodide (PI) and 50 μg/mL RNase. The flow analysis was carried out using a flow cytometer (BD FACSCalibur). Processing and analysis of flow cytometry data were performed on a PC-based computer system.

2.7. Frequency of cell death analysis

Briefly, cell pellets (10^6) were resuspended in 100 μL of a staining solution containing PI, 4,5-diaminofluorescein (DAF) and Hoechst 33258 at the concentration of 0.6, 0.1 and 0.6 mg/mL, respectively. The stained cells were analyzed using a epifluorescence microscope. Samples of 200 cells were analyzed.

2.8. Statistical analysis

Data were analyzed according to analysis of variance (ANOVA) and the Tukey–Kramer multi comparison test *a posteriori*. Two tailed Student's *t*-test was used for the analysis of cell death frequency. Values were considered significant when $p < 0.05$.

3. Results and discussion

The results of the surviving cell fraction as a function of the total physical dose are shown in Fig. 1. The neutron irradiation of the cells showed a decrease in the cell viability. This effect was greater in the cells incubated with the boron compounds (BPA or BOPP). In these studies we evaluated the surviving cell fraction using the MTT colorimetric assay after the treatment with different types of radiation. We have obtained previously similar

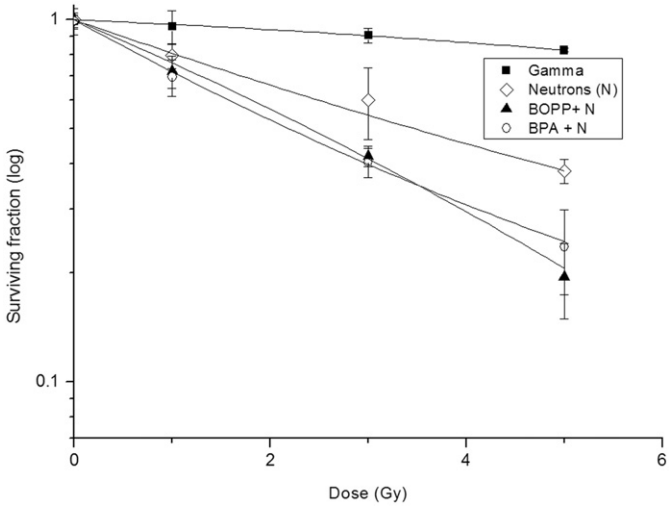

Fig. 1. Survival of WRO cells under the different treatments. Data are fitted with a quadratic-linear model. Each point is the average of 6–8 wells ± SEM of two independent experiments.

results between the clonogenic assay and this particular colorimetric assay, in the physical doses obtained in these experiments, in agreement with other authors (Watts et al., 1989; Slavotinek et al., 1994).

Fig. 2a–c shows an increase of p53 at 24 h for the neutrons alone and gamma groups compared to the control group (without irradiation and without boron compounds). Also it was observed that controls of boron compounds (without irradiation) have an increased expression of p53 (Fig. 2b and c). It was reported that WRO cell line expresses the mutated p53 protein (Namba et al., 1995). It is known that the lack of normal p53 function may cause a failure in the cellular response to DNA damage. The levels of mutated p53 protein were abundant without irradiation and this agrees with other published studies (Torres et al., 2004).

On the other hand, the expression of Ku70 showed an up-regulation of 4 fold in the group irradiated with neutrons alone compared to control group (without irradiation) at 24 h. Also at this time the relative amount of Ku70 increased for the BPA+N group, 1.16 times compared to its respective control (CBPA) and decreases 1.6 times for the BOPP+N group compared to its control (CBOPP). However at 48 h an up-regulation of Ku70 for gamma and BOPP+N groups was observed. The relative amount increased 1.3 times for the gamma group and 1.13 times for BOPP+N (Fig. 3a–c). Ku70 is known to play a role in double strand break repair by the NHEJ pathway. A correlation between decreased expression of Ku70 and an increase of sensitization to radiation (Vandersickel et al., 2010) was described. At the times analyzed in these studies we only observed a lower expression on this protein for the BOPP+N group at 24 h, but further studies are required in order to establish the role of Ku70 in the BNCT treatment.

Accumulation of cells in G2/M was observed at both time points for all the irradiated groups (Table 1). The arrest in G2/M could be a period of time for DNA repair by the studied mechanism. It is known that tumor cells of thyroid that have mutated p53, arrest in G2 after irradiation, independently of the quality of radiation (Namba et al., 1995). On the other hand, the control groups, those which were incubated with boron compounds and were not irradiated, showed an arrest at 24 h. However in these groups, the number of apoptotic and necrotic cells did not increase results not shown and the ATM (for ataxia-telangiectasia mutated) protein did not show an up-regulation at these times, indicating that there was no damage in the cells induced by the boron compounds (results not shown). The ATM protein in the presence of DNA double strand break damage becomes activated and phosphorylates different downstream targets, which act as

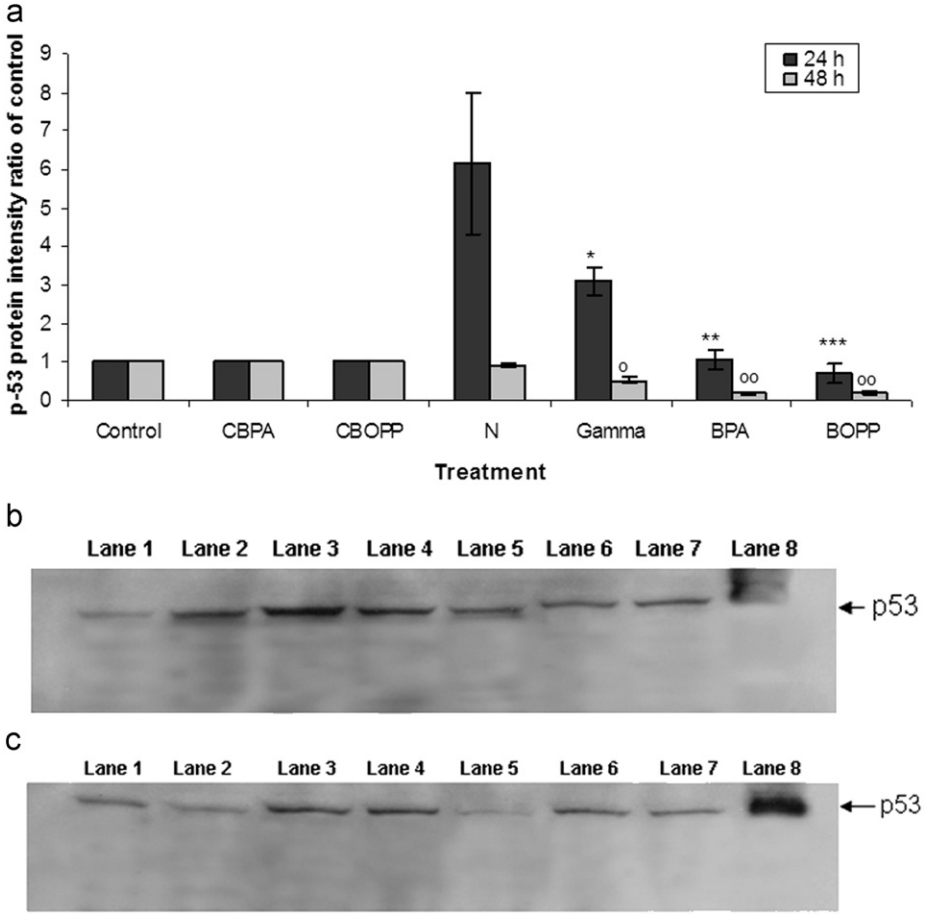

Fig. 2. (a) Expression of p53 was assessed by western blot analysis. All the cells received 3 Gy of total physical absorbed dose and the analysis was performed at 24 and 48 h. Each displayed value was normalized against the density of the respective band of Beta-Actin and the levels of relative optical density are expressed as the ratio between each treatment and its respective control. $^{*}p<0.05$, $^{**}p<0.01$ and $^{***}p<0.001$ for Neutrons vs Gamma, BPA+N and BOPP+N groups, respectively, at 24 h. $^{\circ}p<0.05$ for Neutrons vs Gamma and Gamma vs BPA+N and BOPP+N groups; $^{\circ\circ}p<0.01$ for Neutrons vs BPA+N and BOPP+N groups, at 48 h. (b) Quantitative analysis of proteins by densitometric scanning of the membranes was performed at 24 h. The western blot was performed twice. Lane 1: Control (without irradiation); Lane 2: CBPA; Lane 3: CBOPP; Lane 4: Neutrons; Lane 5: Gamma; Lane 6: N+BPA; Lane 7: N+BOPP; and Lane 8: Molecular weight marker. Beta-Actin was used as the loading control. (c) Quantitative analysis of proteins by densitometric scanning of the membranes was performed at 48 h. The western blot was performed twice. Lane 1: Control (without irradiation); Lane 2: CBPA; Lane 3: CBOPP; Lane 4: Neutrons; Lane 5: Gamma; Lane 6: N+BPA; Lane 7: N+BOPP; and Lane 8: Molecular weight marker. Beta-Actin was used as the loading control.

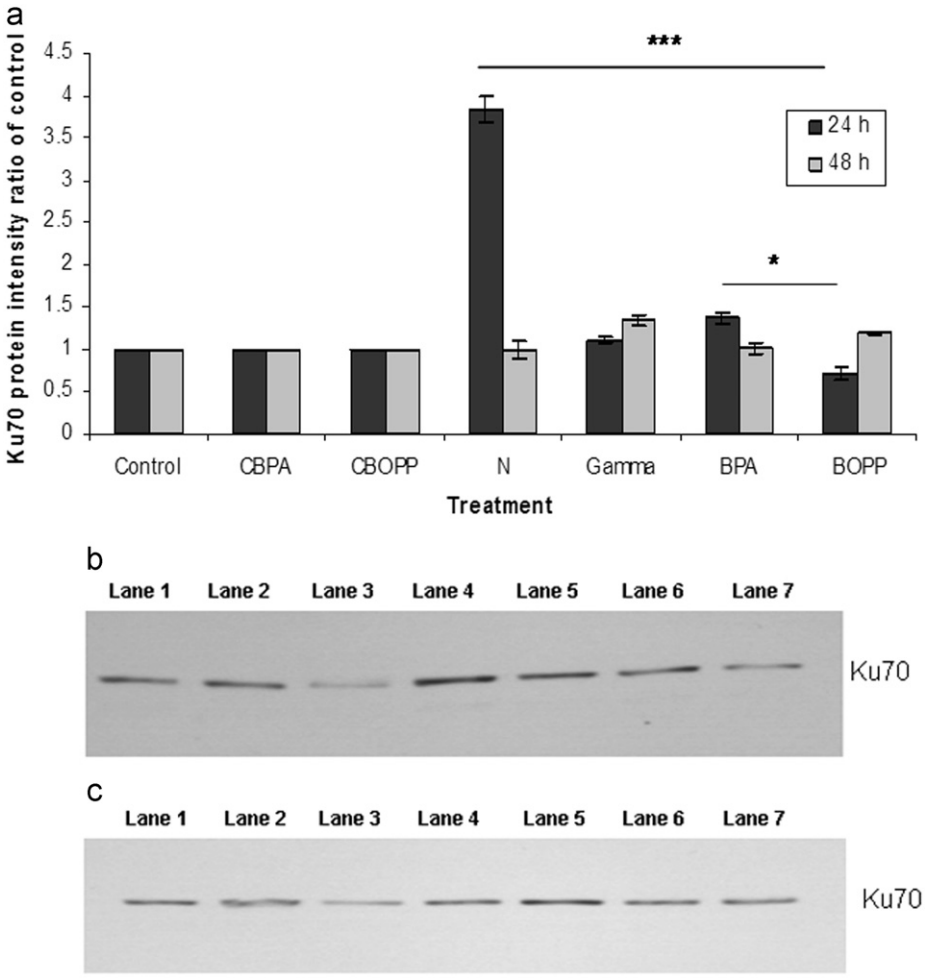

Fig. 3. (a) Expression of Ku70 was assessed by western blot analysis. All the cells received 3 Gy of total physical absorbed dose and the analysis was performed at 24 and 48 h. Each displayed value was normalized against the density of the respective band of Beta-Actin and the levels of relative optical density are expressed as the ratio between each treatment and its respective control. $^{***}p < 0.001$ for Neutrons vs Gamma, BPA+N and BOPP+N groups; $^{*}p < 0.05$ for BPA+N vs BOPP+N groups, at 24 h. (b) Quantitative analysis of proteins by densitometric scanning of the membranes was performed at 24 h. The western blot was performed twice. Lane 1: Control (without irradiation); Lane 2: CBPA; Lane 3: CBOPP; Lane 4: Neutrons; Lane 5: Gamma; Lane 6: N+BPA; and Lane 7: N+BOPP. Beta-Actin was used as the loading control. (c) Quantitative analysis of proteins by densitometric scanning of the membranes was performed at 48 h. The western blot was performed twice. Lane 1: Control (without irradiation); Lane 2: C+BPA; Lane 3: C+BOPP; Lane 4: Neutrons; Lane 5: Gamma; Lane 6: N+BPA; and Lane 7: N+BOPP. Beta-Actin was used as the loading control.

Table 1
Cell cycle analyses.

Group	Time (h)	G1	G2	S
C	24	79.48 ± 14.33	3.31 ± 1.19	17.2 ± 5.55
C	48	77.32 ± 17.39	4.49 ± 0.89	18.17 ± 5.43
C BPA	24	44.07 ± 2.79	19.01 ± 1.6	37.02 ± 4.38
C BPA	48	77.26 ± 4.35	3.09 ± 0.05	19.65 ± 3.2
C BOPP	24	42.75 ± 2.82	16.8 ± 4.03	42.86 ± 1.21
C BOPP	48	66.49 ± 6.23	1.94 ± 0.06	31.57 ± 7.3
Gamma	24	48.38 ± 3.56	17.83 ± 1.55	31.36 ± 2.01
Gamma	48	45.87 ± 15.49	18.72 ± 8.9	33.78 ± 6.57
N	24	53.36 ± 5.18	12.46 ± 1.63	34.17 ± 3.83
N	48	41.54 ± 12.2	16.93 ± 6.89	31.36 ± 11.29
BPA+N	24	63.3 ± 10.18	11.04 ± 0.13	25.53 ± 10
BPA+N	48	67.35 ± 6.87	7.55 ± 3.61	24.81 ± 3.3
BOPP+N	24	61.52 ± 3.85	8.37 ± 2.87	30.01 ± 0.96
BOPP+N	48	54.38 ± 8.18	16.72 ± 5.08	28.83 ± 3.06

Percentage of cells in the various cell phases is shown for each sample (values are mean ± SD). Three independent experiments were performed.

signal transducers and effectors initiating cell cycle arrest and apoptosis (Niida and Nakanishi, 2006).

The study of the mechanisms of cell death showed that at 24 h the frequency of apoptosis was increased in all irradiated groups compared to control groups ($^{**}p < 0.01$ for Neutrons vs Control and $^{*}p < 0.05$ for N+BPA and N+BOPP vs CBPA and CBOPP, respectively). The number of necrotic cells was higher only in all BNCT groups compared to gamma and control groups ($p < 0.05$ for all BNCT groups vs Controls). At 48 h an increase in apoptotic cells in all the groups irradiated ($^{**}p < 0.01$ and $^{*}p < 0.05$ for Neutrons and Gamma groups vs Control, respectively; $^{**}p < 0.01$ for N+BPA vs CBPA) was observed. However the necrotic cells only increased in the groups irradiated with neutrons (Groups 1, 2 and 3) ($^{**}p < 0.01$ for Neutrons and N+BPA groups vs Control and CBPA, respectively). These studies showed that necrosis was the principal mechanism of cell death induced by boron neutron capture therapy.

4. Conclusions

These results performed on follicular thyroid carcinoma cells suggest a different cellular response for all the irradiated groups. The results of the surviving cell fraction showed a decrease in the cell viability for the cells incubated with both boron compounds (BPA or BOPP). The protein p53 showed an up-regulation for the gamma and neutrons groups alone at 24 h after irradiation, which

would not seem to be correlated with the p53-dependent G1/S cell cycle arrest. Cell cycle analysis showed that neutrons, neutrons plus boron compounds and gamma irradiation induced a G2/M arrest at 24 and 48 h after irradiation. We found that cell death was mostly produced by cell necrosis in groups irradiated with neutrons alone and with neutrons and boron compounds, with higher values at 24 h. All the groups irradiated with gamma or neutrons seem to induce the NHEJ repairs system, as evidenced by an increase of Ku70 at different times. The decrease of Ku70 in the BNCT (neutrons+BOPP) group could play a role in the increase of sensitization to radiation.

Conflict of interest statement

We declare that there is no conflict of interest in this paper.

Acknowledgments

The present studies were performed with grants from the National Research Council of Argentina (CONICET), the National Agency for Scientific and Technological Promotion (ANPCYT), and the University of Buenos Aires. We also thank Dr. Sara Liberman (National Atomic Energy Commission) for her continuous support.

References

Altieri, S., Bortolussi, S., Barth, R.F., Roveda, L., Zonta, A., 2009. 13th International Congress on Neutron Capture Therapy. BNCT: a new option against cancer. Appl. Radiat. Isot. 67 (7–8 Suppl.), S1–S2.

Coderre, J.A., Morris, G.M., 1999. The radiation biology of boron neutron capture therapy. Radiat. Res. 151 (1), 1–18.

Dagrosa, M.A., Viaggi, M., Longhino, J., Calzetta, O., Cabrini, R., Edreira, M., Juvenal, G., Pisarev, M., 2003. Experimental application of boron neutron capture therapy (BNCT) to undifferentiated thyroid carcinoma (UTC). Int. J. Radiat. Oncol. Biol. Phys. 57 (4), 1084–1092.

Dagrosa, M.A., Thomasz, L., Longhino, J., Perona, M., Calzetta, O., Blaumann, H., Jiménez Rebagliati, R., Cabrini, R.L., Kahl, S.B., Juvenal, G.J., Pisarev, M.A., 2007. Optimization of the application of boron neutron capture therapy (BNCT) to the treatment of undifferentiated thyroid cancer (UTC). Int. J. Radiat. Oncol. Biol. Phys. 69 (4), 1059–1066.

Dagrosa, M.A., Crivello, M., Perona, M., Thorp, S., Santa Cruz, G.A., Pozzi, E., Casal, M., Thomasz, L., Cabrini, R., Kahl, S., Juvenal, G.J., Pisarev, M.A., 2011. First evaluation of the relative biological effectiveness of boron neutron capture therapy (BNCT) in a colon carcinoma cell line. Int. J. Radiat. Oncol. Biol. Phys. 79 (1), 262–268.

Kato, I., Fujita, Y., Maruhashi, A., Kumada, H., Ohmae, M., Kirihata, M., Imahori, Y., Suzuki, M., Sakrai, Y., Sumi, T., Iwai, S., Nakazawa, M., Murata, I., Miyamaru, H., Ono, K., 2009. Effectiveness of boron neutron capture therapy for recurrent head and neck malignancies. Appl. Radiat. Isot. 67, S37–42.

Miller, M., Quintana, J., Ojeda, J., Langan, S., Thorp, S., Pozzi, E., Sztejnberg, M., Estryk, G., Nosal, R., Saire, E., Agrazar, H., Graiño, F., 2009. New irradiation facility for biomedical applications at the RA-3 reactor thermal column. Appl. Radiat. Isot. 67, S226–S229.

Namba, H., Hara, T., Tukazaki, T., Migita, K., Ishikawa, N., Ito, K., Nagataki, S., Yamashita, S., 1995. Radiation induced G1 arrest is selectively mediated by the p53-WAF1/Cip1 pathway in human thyroid cells. Cancer Res. 55, 2075–2080.

Niida, H., Nakanishi, M., 2006. DNA damage checkpoints in mammals. Mutagenesis 21 (1), 3–9.

Norppa, H., Falck, G., 2003. What do human micronuclei contain? Mutagenesis 18 (3), 221–223.

Ochi, T., Sibanda, B.L., Wu, Q., Chirgadze, D.Y., Bolanos-Garcia, V.M., Blundell, T.L., 2010. Structural biology of DNA repair: spatial organization of the multi-component complexes of nonhomologous end joining. J. Nucleic Acids 25, 621–695.

Pawlik, T.M., Keyomarsi, K., 2004. Role of cell cycle in mediating sensitivity to radiotherapy. Int. J. Radiat. Oncol. Biol. Phys. 59 (4), 928–942.

Slavotinek, A., McMillan, T.J., Steel, C.M., 1994. Measurement of radiation survival using the MTT assay. Eur. J. Cancer 30, 1376–1382.

Torres, M., Muneera, A.B., Ghazi, A., 2004. Induction of p53 and p21 proteins by gamma radiation in skin fibroblasts derived from breast cancer patients. Int. J. Radiat. Oncol. Biol. Phys. 58 (2), 479–484.

Vandersickel, V., Mancini, M., Slabbert, J., Marras, E., Thierens, H., Perletti, G., Vral, A., 2010. The radiosensitizing effect of Ku70/80 knockdown in MCF10A cells irradiated with X-rays and p(66)+Be(40) neutrons. Radiat. Oncol. 5, 30.

Watts, M.E., Roberts, I.J., Wood Cock, M., 1989. A comparison of colorimetric and clonogenic assay for hypoxic-specific toxins with hamster and human cells. Int. J. Radiat. Oncol. Biol. Phys. 16 (4), 939–942.

Wittig, A., Collette, L., Appelman, K., Bührmann, S., Jäckel, M.C., Jöckel, K.H., Schmid, K.W., Ortmann, U., Moss, R., Sauerwein, W.A., 2009. EORTC trial 11001: distribution of two 10B-compounds in patients with squamous cell carcinoma of head and neck, a translational research/phase 1 trial. J. Cell Mol. Med. 13, 1653–1665.